

Parametric investigation and analysis of fishnet metamaterials in the microwave regime

N.-H. Shen,^{1,*} G. Kenanakis,¹ M. Kafesaki,^{1,2} N. Katsarakis,^{1,3} E. N. Economou,^{1,4} and C. M. Soukoulis^{1,2,5}

¹*Institute of Electronic Structure and Laser (IESL), Foundation for Research and Technology-Hellas (FORTH), 71110 Heraklion, Crete, Greece*

²*Department of Materials Science and Technology, University of Crete, 71003 Heraklion, Crete, Greece*

³*Science Department, Technological Educational Institute of Crete, 71004 Heraklion, Crete, Greece*

⁴*Department of Physics, University of Crete, 71003 Heraklion, Crete, Greece*

⁵*Ames Laboratory-USDOE, and Department of Physics and Astronomy, Iowa State University, Ames, Iowa 50011, USA*

*Corresponding author: nhshen@iesl.forth.gr

Received August 3, 2009; accepted August 18, 2009;
posted August 25, 2009 (Doc. ID 115131); published September 29, 2009

We study through experiments and associated simulations the electromagnetic response of microwave fishnet metamaterials and its dependence on the system's geometrical parameters. Our study verifies the validity of an earlier proposed inductor-capacitor (LC) circuit description of the fishnet design and reveals a left-handed response with high transmittance for a wide variety of geometrical structure parameters. This study paves the way to achieve optimized left-handed fishnet metamaterial designs. © 2009 Optical Society of America
OCIS codes: 160.3918, 120.7000, 120.4530.

1. INTRODUCTION

Metamaterials are a special category of artificially engineered structures with subwavelength unit cells. In recent years, research on metamaterials, especially on left-handed materials (LHMs, i.e. metamaterials with simultaneously negative electrical permittivity, ϵ , and magnetic permeability, μ), has aroused much interest due to the many involved intriguing physical properties such as negative refraction [1–3], and practical potential applications such as the subdiffraction-limited planar lens [3–6].

Doubtlessly, the development of research on metamaterials is tightly connected with structure design. As is well known, the difficulty in finding natural materials showing negative permeability is the reason that Veselago's hypothesis on LHMs [1] had been given a cold shoulder for more than 30 years until the first realistic left-handed (LH) structure in a microwave regime [2] came out; the unit cell of this structure was actually a combination of thin metallic wires leading to $\epsilon < 0$ [7] and split-ring resonators (SRRs) leading to $\mu < 0$ [8], both proposed theoretically by Sir J. Pendry. Afterwards, many novel metamaterial designs, especially designs showing negative permeability, were proposed aiming at more simplified fabrication and testing processes, lower intrinsic losses, and operation at higher frequencies, even the visible regime [9–14].

During these metamaterial studies, an important forward step was started from the work by Podolskiy *et al.* [15], in which a resonant magnetic response leading to negative permeability values was achieved using pairs of short slabs (or wires) instead of SRRs. In contrast to the in-plane incidence required to demonstrate the magnetic response in SRRs, the short-slab pair-based designs show

a magnetic response for normal incidence; thus, even a single functional layer sample can be used to demonstrate this response. Moreover, the design allows a much more simplified fabrication and characterization procedure than the SRRs-based designs. That is why many of today's LHMs, especially in the μm and sub- μm scales, are based on the short-slab pair design. Among these materials, a structure with a superior performance seems to be the so-called fishnet structure [16–19] (see Fig. 1), which is composed of wide-slab pairs (responsible for the negative μ response) physically connected with continuous wires (responsible for the negative ϵ response). Detailed numerical analysis of the fishnet design in the microwave regime [20] has revealed a left-handed response with high transmittance for quite a broad range of geometrical structure parameters. This improved response was attributed to the large width of the slabs (w_s), together with the physical connection of slabs and wires. The large width of the slabs allows for a large volume of the induced magnetic field and thus for a strong magnetic response; moreover, in synergy with the connection of slabs and wires, it pushes the lower resonant electric mode of the structure much above the magnetic resonance regime, leading to a smooth, nonresonant $\epsilon(\omega)$ response at the magnetic resonance and thus to the possibility for a broadband good impedance match with the environment. The superior behavior of the fishnet design is suggested also by the fact that all the currently achieved μm - and sub- μm -scale LHMs are based on the fishnet design [21]. Quite recently, a multilayer LHM in the optical regime has been successfully obtained using a fishnet [22], which allowed for the first experimental negative refraction demonstration of propagating waves in the optical regime.

Since fishnet seems to be an optimized design for

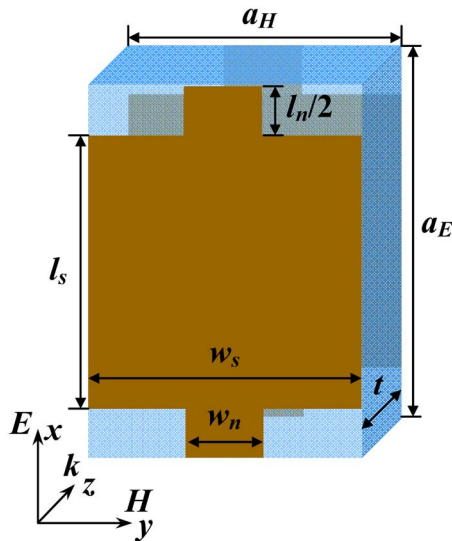


Fig. 1. (Color online) Schematic of the unit cell of the fishnet structure. \mathbf{E} , \mathbf{H} , and \mathbf{k} correspond to electric field, magnetic field, and wave vector, respectively. a_E and a_H are the x and y size of unit cells, respectively. l_s is the length of the slabs, w_s the width of the slabs, w_n the width of the continuous wires (necks), l_n the length of the neck parts, and t the thickness of the dielectric substrate.

achievement of LHMs, it is very important to investigate it in detail and to be able to predict the electromagnetic (EM) response of this design as a means to tailor the properties of the design. Moreover, since most of the current conclusions on the fishnet design are based on results of simulations, it is important to validate experimentally these conclusions and the existing models describing the fishnet. One such model that has been proposed earlier by our group [20] uses a simplified LC circuit description to predict the dependence of the EM response of the fishnet on the geometry and topology. Some other theoretical analyses were followed, seeing the structure from different viewpoints [23,24]; they interpreted negative magnetic permeability to be a result in the excitation of gap surface plasmon polariton modes in the dielectric film, while electric permittivity is considered to be governed by the cutoff frequency of the hole waveguide. However, neither related experimental results nor detailed simulations were presented there to validate the predictions of the analytical models.

In this research, we shall revisit the parametric study of microwave fishnet metamaterials, providing results from both experiments and simulations that consolidate the analyses and verify the predictions of the LC circuit description proposed in [20]. In parallel, we use this LC circuit description to analyze the achieved experimental response. Hence, we can obtain a distinct and intuitive understanding of the parametric response of fishnet metamaterials, which can lead to guidelines for optimization of the fishnet and related metamaterial structures.

2. THEORETICAL AND EXPERIMENTAL INVESTIGATIONS OF THE FISHNET STRUCTURES

In this section we will first review the EM response of the fishnet structure as predicted by a simple LC circuit de-

scription of the structure [20]. After that, we will present both experimental and simulation results for different geometrical and topological parameters of the structure, examining the validity and the areas of applicability of the LC circuit model.

A. LC Circuit Model for the Fishnet and its Predictions

As it was mentioned in the Introduction, the fishnet structure can be treated as a physically connected combination of short-slab pairs, which are contiguous along \mathbf{H} direction, and continuous wires, which are along \mathbf{E} direction (see Fig. 1). According to [20], at the magnetic resonance of the fishnet structure at a frequency ω_m , not only are the currents at the slab pair antiparallel, forming a loop-current (just like for short-slab pairs only), but the currents at the neck parts (which join slabs along \mathbf{E} direction) are also antiparallel, forming another loop current opposite to the one of the slabs, which contributes to the magnetic response of the structure. Snapshots of the fields and currents at the magnetic resonance suggest that this contribution can be taken into account in an effective LC circuit model of the structure by considering the loop inductance of a neck, L_n , in parallel to the one of the slabs, L_s , such as

$$\omega_m^2 = \frac{1}{LC} = \frac{1}{L_s C} + \frac{1}{L_n C} \approx \omega_{m,\text{slabs}}^2 + \frac{1}{L_n C}. \quad (1)$$

In Eq. (1) C is the capacitance between the slabs of the pair and $\omega_{m,\text{slabs}}$ is the magnetic resonance frequency of the slab pairs only structure. The symbol \approx at the right-hand side of Eq. (1) is used because the inductance and the capacitance of the isolated (nonconnected) slab pairs (and thus $\omega_{m,\text{slabs}}$) are slightly different than those of the fishnet, L_s and C .

Besides the magnetic response of an LH system, its electric response [described by $\epsilon(\omega)$] is also very important; it plays a crucial role in determining the possibility of achieving a left-handed (LH) frequency band with good impedance match to free space leading to high LH transmittance. As is shown in [25], the introduction of the magnetic components such as SRRs and short-slab pairs in a thin-wires system leads to a severe modification of the plasma frequency of the continuous wires, ω_p . Generally, the total plasma frequency of LHMs, ω_p' , shall be essentially determined by the electric dipole-like resonance frequency of the magnetic structures, which in most of the cases lies below the wire plasma frequency; the effect of this dipole-like resonance is a strong downwards shift of the plasma frequency and an abrupt slope of the $\epsilon(\omega)$ curve at ω_p' , which are both undesired effects for achievement of LHMs with a good impedance match with their environment. These effects seem to be minimized in fishnet, as it is suggested by an additional LC circuit description of the structure, now close to the structure dipole-like electric resonance frequency [20,26], ω_e .

Again, due to the antiparallel currents in slabs and necks at the electric resonance frequency, the effective inductance of the necks L_n' will be still in parallel with the slab inductance L_s' , so

$$\omega_e^2 = \frac{1}{L'C'} = \frac{1}{L'_s C'} + \frac{1}{L'_n C'} \approx \omega_{e,\text{slabs}}^2 + \frac{1}{L'_n C'}. \quad (2)$$

In Eq. (2) L'_s denotes the straight-wire inductance of the slabs of the pair and L'_n the one of the necks, while C' is the capacitance between neighboring slabs along the external \mathbf{E} direction and $\omega_{e,\text{slabs}}$ is the electric resonance frequency of only the slabs.

Equation (2) shows that the electric resonance frequency of the fishnet structure is higher than that of the slabs only, which is already higher than the magnetic resonance frequency due to the large width of the slabs, which leads to small inductance L'_s , and thus it is expected to have an insignificant effect on the plasma frequency of the total system, ω_p' , which is essentially determined by the plasma frequency of only the continuous wires.

Using qualitative relations connecting the capacitances and inductances of Eqs. (1) and (2) with the geometrical parameters of the structure, it is easy to obtain the geometric dependence of the frequencies ω_m and ω_e of the fishnet structure within the LC circuit framework.

Since we want to restrict this to just a qualitative description, it is sufficient to employ the parallel plate capacitor formula for capacitance C of the slabs and the solenoid inductor description for the loop inductances, i.e.,

$$C \sim \frac{w_s l_s}{t}, \quad \text{and} \quad L_s \sim \frac{l_s t}{w_s}, \quad L_n \sim \frac{l_n t}{w_n}, \quad (3)$$

where w_s and w_n are the widths of slabs and necks, respectively, while l_s and l_n are the corresponding lengths (see Fig. 1). Using Eqs. (3), the magnetic resonance frequency appears to have a qualitative behavior of the form

$$\omega_m \sim \sqrt{\frac{A}{l_s^2} + \frac{1}{l_s l_n} \frac{w_n}{w_s}}, \quad (4)$$

with A as constant.

Concerning the qualitative geometric dependence of the electric resonance frequency ω_e , it can result by approximating the capacitance C' with that between two parallel wires of length w_s and radius t_m , i.e.,

$$C' \sim w_s / \ln(b/t_m), \quad (5)$$

where b is the separation between the wires (in our case equal to l_n) [20,26] and the inductances L'_s, L'_n by formulas appropriate for a straight-wire inductance, i.e.,

$$L'_s \sim l_s \ln(l_s/w_s), \quad L'_n \sim l_n \ln(l_n/w_n). \quad (6)$$

Then, the electric resonance frequency takes the form

$$\omega_e^2 \sim \frac{\ln(b/t_m)}{w_s} \left[\frac{B}{l_s \ln(l_s/w_s)} + \frac{D}{l_n \ln(l_n/w_n)} \right], \quad (7)$$

where B and D are constants determined by other parameters of the system.

Equations (4) and (7) show the dependence of the magnetic and electric resonance frequencies on the system parameters. In the following, we will investigate the validity of these formulas, both experimentally and theoretically, by transmission spectra through fishnet slabs.

B. Experimental and Theoretical Investigations of Realistic Fishnet Structures

In this section we present and discuss theoretical (simulation) and experimental transmission data for the fishnet design, examining the effect on the transmission of the various geometrical parameters of the design. Specifically, we examine the effect on the transmission spectra of the width of the neck parts of the fishnet (w_n), the width of the slab parts (w_s), the length of the slabs (l_s), the lattice constant along propagation direction a_k , and number of unit cells along the propagation direction. Also, we investigate and propose an isotropic fishnet design able to give LH behavior for all possible incident polarizations.

The experimental structures studied here have been fabricated using standard printed circuit board technology with double-faced copper patterns of thickness $t_m = 30 \mu\text{m}$ patterned on FR4 dielectric boards of thickness $t = 1.6 \text{ mm}$. The samples possess 13 and 18 unit cells (u.c.) along the directions of the external electric field and the magnetic field, respectively.

The characterization of the samples has been done through free-space transmission measurements using an HP 8722 ES network analyzer and a pair of microwave standard-gain horn antennas as source and receiver. Regarding the simulations, they have been performed through the well-established commercial software CST Microwave Studio, which is based on the finite integration technique. Both input and output waveguide ports away from the sample serve as source and receiver; periodic boundary conditions at the lateral directions are adopted to mimic the experimental configuration. The conductivity of the copper has been taken as $5.8 \times 10^7 \text{ S/m}$, the dielectric constant of the board as 4, and electric conductivity of the board as 0.08 S/m . For verification of the left-handed behavior of our structures we may use the standard retrieval procedure of calculating the effective structure parameters ϵ and μ from transmission and reflection data through a homogeneous medium approximation of the actual structures [27].

In our analysis, we will set the following geometrical parameters as a basis (i.e., as basic system on which we will examine the effect of parameter changes): $a_E = 9.5 \text{ mm}$, $a_H = 7 \text{ mm}$, $a_k = 3.1 \text{ mm}$, $l_s = 7 \text{ mm}$, $w_s = 7 \text{ mm}$, $t = 1.6 \text{ mm}$, $t_m = 30 \mu\text{m}$, $w_n = 2 \text{ mm}$, and 3 layers along propagation direction. The experimental and simulation transmission results for the basis parameters are shown in Fig. 2 (dotted lines). The high transmittance band around 13 GHz is proved [20] to possess LH properties and is slightly above the magnetic resonance frequency of the slabs-only case [20], which falls at $\sim 11 \text{ GHz}$.

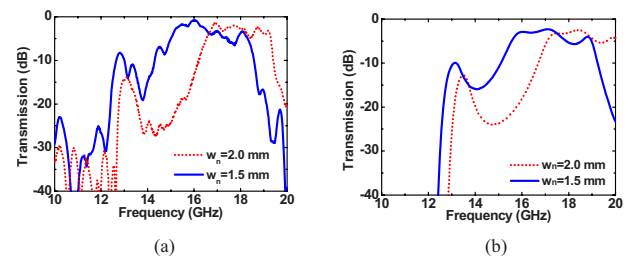


Fig. 2. (Color online) (a) Experimental and (b) simulated transmission spectra for fishnet structures with different width of necks. Solid lines, $w_n = 1.5 \text{ mm}$; dotted lines, $w_n = 2 \text{ mm}$.

1. Role of the Neck Width (w_n)

Reducing the width of the necks (w_n) in our basis system from 2 mm to 1.5 mm and examining the resulting transmission properties we obtain what is observed in Fig. 2 (dotted lines). Figure 2(a) shows the measured transmission results and Fig. 2(b) shows the corresponding simulation data, in quite good agreement with the experimental ones. It can be seen from Fig. 2 that the decrease of w_n leads to decrease of both ω_m and ω_e (the spectral position of ω_e is indicated by the transmission dip at ~ 20 GHz, due to negative ϵ and positive μ), as well as of the system plasma frequency ω_p' . The decrease of both ω_m and ω_e can be easily predicted by the LC circuit model through Eqs. (4) and (7), respectively.

The physical mechanism behind the decrease of ω_m can be understood more by reviewing Eqs. (1) and (3): decrease of w_n leads to increase of the neck loop inductance, decreasing thus the neck's contribution to the magnetic resonance frequency as discussed in [20] and indicated also by Eq. (2); the contribution of the neck's loop inductance results to an upwards shift of the magnetic resonance frequency, compared to that of the slab-pairs only. The same also hold for the electric resonance frequency. The downwards shift of the plasma frequency by decreasing the neck width is here mostly due to the decrease of the continuous wire's plasma frequency in the fishnet (thinner wires in a continuous wire system lead to lower plasma frequency values due to the lower density of electrons and to larger magnetic field inductance [7]). It is noticed from Fig. 2 that the neck's width is an essential parameter, which determines the separation between the LH band and right-handed (RH) regime, a critical factor for the impedance of the structure.

2. Role of the Slab Width (w_s)

In the original fishnet design the width of the metallic slabs is equal to the lattice constant along the \mathbf{H} direction, leading to contiguous slabs. It is interesting though to examine the effect of reducing this width (keeping the unit cell unchanged) leading to a modified fishnet design, where slab pairs are not contiguous anymore along the \mathbf{H} direction. This modified design has the advantage that it is more appropriate for creating two-dimensional systems where mutually perpendicular structure planes need to cross each other.

Reducing the slab width from $w_s = 7$ mm (as in our basis system) to $w_s = 5$ mm, we obtain the transmission result shown in Fig. 3 (solid line). Figure 3(a) shows the experimental result and Fig. 3(b) the corresponding theoretical

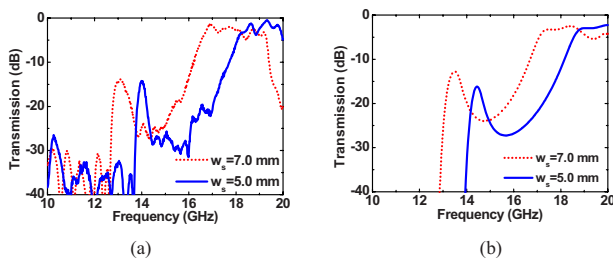


Fig. 3. (Color online) (a) Experimental and (b) simulated transmission spectra for fishnet structures of different slab widths. Solid line, $w_s = 5$ mm; dotted line, $w_s = 7$ mm.

result, in good agreement with the experiment as far as the position of the characteristic structure frequencies. Both experimental and simulation results show a distinct increase of the magnetic resonance frequency by decreasing w_s . This increase agrees well with what can be predicted from Eq. (4). For understanding this effect we should look again at Eq. (1). Equation (1), in combination with Eqs. (3), suggest that while in isolated (not connected) slab pairs the width of the slabs does not affect their magnetic resonance frequency a lot (reduction of width results in an increase of the slab inductance, which is compensated by an analogous decrease of the capacitance, C), in the fishnet the coupling between slabs and necks makes this parameter have a considerable influence, since in fact what determines the neck's influence is not the neck inductance itself but its ratio to the slab inductance. This can be seen more clearly by writing Eq. (1) as $\omega_m^2 = (1/L_s C)(1 + L_s/L_n)$ and taking into account that a decrease of the slab's width results in an increase of the slab's loop inductance [see Eq. (3)].

Besides the increase of ω_m , the decrease of the slab width seems to result also in an increase of the system plasma frequency. This increase of the plasma frequency seems to be a result of both the increased electric resonance frequency of the slabs, $\omega_{e,slabs}$ due to increased slab straight-wire-type inductance, L_s' [see Eq. (6)] and the decreased average width of the continuous-wire component of the structure in an analogous way as explained in the previous paragraph.

3. Role of the Slab Length (l_s)

When we consider an increase of the length of the slabs, Eqs. (4) and (7) predict a decrease of both electric and magnetic resonance frequencies of the system. This decrease is indeed observed in Fig. 4, where we show experimental [Fig. 4(a)] and simulation [Fig. 4(b)] data for a structure where l_s is equal to 8 mm and compare them with the transmission of our basis system of $l_s = 7$ mm. The decrease of the electric resonance frequency is more clear in the experimental data (see the dip at ~ 20 GHz); the slight difference between theoretical and experimental data in the estimation of the electric resonance frequency is, most probably, a result of a nonuniformity in the dielectric constant of the board.

One way to understand this decrease of both ω_m and ω_e by increasing the slab length is if we consider the electric and magnetic resonance of the pair as the antisymmetric and symmetric modes resulting from the coupling of the two single-slab dipole resonances in the pair. The wave-

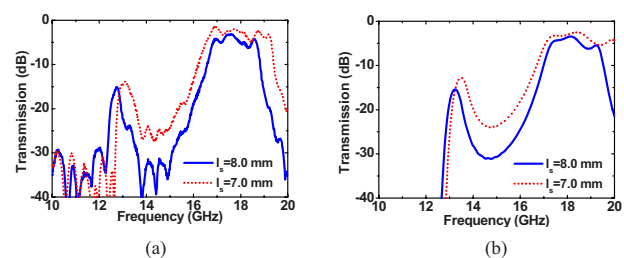


Fig. 4. (Color online) (a) Experimental and (b) simulated transmission spectra of fishnet structure for different lengths of slabs. Solid line, $l_s = 8$ mm; dotted line, $l_s = 7$ mm.

length of the single-slab dipole resonance increases with the length of the slab, leading to a decrease of the resonance frequency.

Despite the above-mentioned decrease of the electric resonance frequency, we observe a slight upwards shift of the system plasma frequency by increasing the slab length. This upwards shift seems to come from the contribution of the straight-wire component of the structure, which gets a larger average width and thus an increased plasma frequency.

4. Isotropic Fishnet Structure

Another modified structure to the originally proposed fishnet design is the so-called isotropic-like fishnet [20], the unit cell of which is shown in Fig. 5. The advantage of this design is that, since it has in-plane symmetry, it works the same way for external electric field polarizations along both x and y directions. Thus, it can demonstrate LH response for unpolarized incident waves as well, assuming propagation along the z direction. In contrast to other proposed isotropic designs with a cross-like shape of the metallic components (see, e.g., [28]) the structure of Fig. 5 has the additional advantage that it has more parameters to tune, and thus one can obtain a more optimized LH behavior.

In Fig. 6 we present both theoretical and experimental data for the design of Fig. 5 (not optimized), and we compare them with the corresponding results of the traditional fishnet with the same unit cell size along \mathbf{E} and \mathbf{k} directions. In the isotropic-like fishnet, the high transmittance frequency band, which is around 13–14 GHz, corresponds to an LH regime, as can be revealed from field and current simulations and effective parameter determination. The difference in the transmission characteristics between the traditional fishnet and the isotropic one can be easily understood using the discussion of the previous paragraphs.

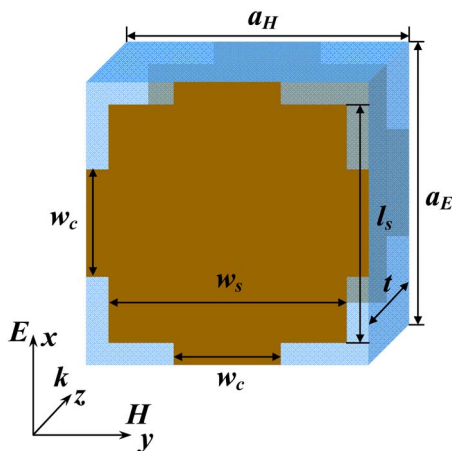


Fig. 5. (Color online) Schematic of the unit cell of an isotropic-like fishnet structure. \mathbf{E} , \mathbf{H} , and \mathbf{k} correspond to electric field, magnetic field, and wave vector, respectively. $a_E=9.5$ mm and $a_H=9.5$ mm are the x and y size of the unit cells, respectively. $l_s=8$ mm is the length of short slabs, $w_s=8$ mm the width of slabs, $w_n=3.6$ mm the width of continuous wires (necks), and $t=1.6$ mm the thickness of the substrate. Thickness of the copper layers is $t_m=30$ μm .

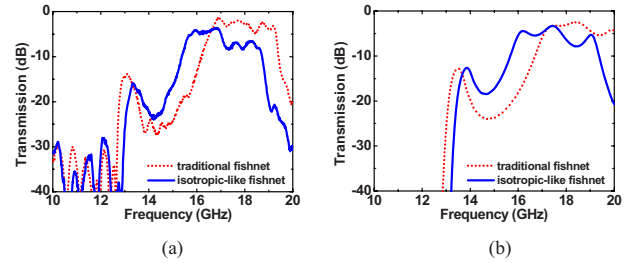


Fig. 6. (Color online) Comparison of transmission spectra between isotropic-like fishnet (solid curve) with parameters shown in Fig. 5 and traditional fishnet (dotted curve) with parameters those of the basis case. (a) Measurements; (b) simulations.

We should mention here that to achieve an isotropic-like LH fishnet design by modifying a traditional LH fishnet, it is essential to perform modification of almost all structure parameters. These modifications can be easily predicted, though, with the help of Eqs. (4) and (7), together with the formula giving the plasma frequency in continuous wire systems [7].

5. Role of the Unit Cells Separation

Besides the above mentioned investigations, we also investigated the transmission spectra for fishnet structures with different unit cell sizes along propagation direction a_k (see Fig. 7). Note that the influence of the unit cell separation is something that cannot be concluded directly by the simple Eqs. (4) and (7), which concern isolated layers and do not take into account any coupling effects between successive layers.

From Fig. 7 one can see that the transmission is enhanced by decreasing a_k , and simultaneously a slight blue-shift effect of the magnetic resonance frequency is observed. Moreover, the plasma frequency is shifted to lower values (due to the increased average metal-density). This plasma frequency shift indicates a change in $\epsilon(\omega)$ and thus a change of the impedance match of the structure with the environment, which is most probably the main reason of the transmission enhancement by the decreasing a_k . The slight magnetic resonance frequency shift can be understood by taking into account that the increased interaction of the unit cells along propagation direction results to a slight decrease of total flux passing through each magnetic resonator and, thus, to a decrease of the effective self-inductance in the description of isolated resonators.

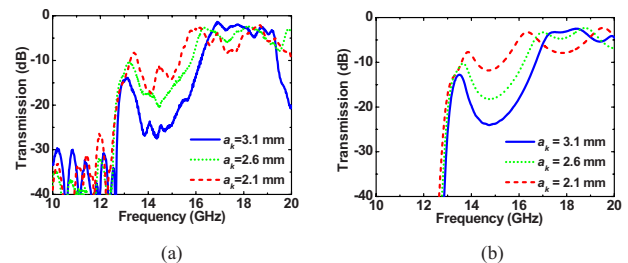


Fig. 7. (Color online) (a) Experimental and (b) simulated transmission spectra of fishnet structure for different sizes of the unit cells along propagation direction, a_k .

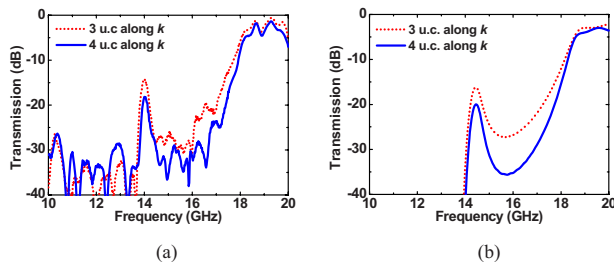


Fig. 8. (Color online) (a) Experimental and (b) simulated transmission spectra of modified fishnet structure with $w_s=5$ mm for different number of unit cells (u.c.) along propagation direction.

6. Changing the Number of Layers

Finally, we also performed both measurements and simulations for cases with different number of layers along the propagation direction but for the modified fishnet structure with $w_s=5$ mm. This is mostly to examine the relative influence of resistive losses and impedance mismatch in the reduction of the LH transmission intensity. The results are shown in Fig. 8, where it can be seen that the LH frequency regime is kept independent of the number of layers, while the transmitted intensity in the experimental data decreases by ~ 3 dB with the incorporation of an additional unit cell (layer). This 3 dB-per-unit cell loss is clearly due to the poor quality of the dielectric (FR4) involved in our fishnet structures, indicating that a good quality dielectric would be able to give LHMs of high transparency.

3. CONCLUSIONS

We presented a systematic parametric study of the fishnet structure and of some related modified designs, with both measurements and simulations, in quite good agreement with each other. We examined the influence on the transmission results and on the characteristic structure frequencies of the slab width, slab length, neck width, layer spacing, and layer numbers involved. The results of our parametric study can be qualitatively predicted and understood through an LC circuit model of the structure, which also takes into account the inductive response of the neck parts of the fishnet structure at the characteristic structure frequencies. On the other hand, our experimental and simulation results validate this LC circuit model. Finally, an isotropic-like fishnet structure was investigated, which can give LH behavior for nonpolarized incident waves and gives a lot of space for structure optimization due to the multitude of controllable geometrical parameters. This work can be treated as a solid foundation for optimizing fishnet structure aiming at realizing more practical applications within a wide range of frequency regimes.

ACKNOWLEDGMENTS

The authors acknowledge financial support by the European Union (EU) under the projects PHOME FET contract 213390, ENSEMBLE (NMP-STREP), and ECONAM (NMP-CA), and the COST Actions MP0702 and MP0803; and also by the Air Force office of Scientific Research, Air Force Material Command (AFMC), USAF grant FA8655-

07-1-3037. Work at Ames Laboratory was supported by the Department of Energy (Basic Energy Science) under contract DE-ACD2-07CH11358.

REFERENCES

1. V. G. Veselago, "The electrodynamics of substances with simultaneously negative values of ϵ and μ ," *Sov. Phys. Usp.* **10**, 509–514 (1968).
2. R. A. Shelby, D. R. Smith, and S. Schultz, "Experimental verification of a negative index of refraction," *Nature* **292**, 77–79 (1997).
3. J. B. Pendry, "Negative refraction makes a perfect lens," *Phys. Rev. Lett.* **85**, 3966–3999 (2000).
4. N. Fang, H. Lee, C. Sun, and X. Zhang, "Sub-diffraction-limited optical imaging with a silver superlens," *Science* **308**, 534–537 (2005).
5. D. O. S. Melville and R. J. Blaikie, "Super-resolution imaging through a planar silver layer," *Opt. Express* **13**, 2127–2134 (2005).
6. K. Aydin, I. Bulu, and E. Ozbay, "Subwavelength resolution with a negative-index metamaterial superlens," *Appl. Phys. Lett.* **90**, 254102 (2007).
7. J. B. Pendry, A. J. Holden, W. J. Stewart, and I. Youngs, "Extremely low frequency plasmons in metallic mesostructures," *Phys. Rev. Lett.* **76**, 4773–4776 (1996).
8. J. B. Pendry, A. J. Holden, D. J. Robbins, and W. J. Stewart, "Magnetism from conductors and enhanced nonlinear phenomena," *IEEE Trans. Microwave Theory Tech.* **47**, 2075–2084 (1999).
9. S. Linden, C. Enkrich, M. Wegener, J. Zhou, T. Koschny, and C. M. Soukoulis, "Magnetic response of metamaterials at 100 terahertz," *Science* **306**, 1351–1353 (2004).
10. J. Zhou, Th. Koschny, M. Kafesaki, E. N. Economou, J. B. Pendry, and C. M. Soukoulis, "Saturation of the magnetic response of split-ring resonators at optical frequencies," *Phys. Rev. Lett.* **95**, 223902 (2005).
11. L. Ran, J. Huangfu, H. Chen, Y. Li, X. Zhang, K. Chen, and J. A. Kong, "Microwave solid-state left-handed material with a broad bandwidth and an ultralow loss," *Phys. Rev. B* **70**, 073102 (2004).
12. N. Liu, H. Guo, L. Fu, S. Kaiser, H. Schweizer, and H. Giessen, "Three-dimensional photonic metamaterials at optical frequencies," *Nature Mater.* **7**, 31–37 (2008).
13. M. S. Rill, C. Plet, M. Thiel, I. Staude, G. V. Freymann, S. Linden, and M. Wegener, "Photonic metamaterials by direct laser writing and silver chemical vapour deposition," *Nature Mater.* **7**, 543–546 (2008).
14. G. Dolling, C. Enkrich, M. Wegener, J. F. Zhou, C. M. Soukoulis, and S. Linden, "Cut-wire pairs and plate pairs as magnetic atoms for optical metamaterials," *Opt. Lett.* **30**, 3198–3200 (2005).
15. V. A. Podolskiy, A. K. Sarychev, and V. M. Shalaev, "Plasmon modes and negative refraction in metal nanowire composites," *Opt. Express* **11**, 735–745 (2003).
16. R. Ulrich, "Far-infrared properties of metallic mesh and its complementary structure," *Infrared Phys.* **7**, 37–50 (1967).
17. S. Zhang, W. Fan, N. C. Panoiu, K. J. Malloy, R. M. Osgood, and S. R. J. Brueck, "Experimental demonstration of near-infrared negative-index metamaterials," *Phys. Rev. Lett.* **95**, 137404 (2005).
18. S. Zhang, W. Fan, K. J. Malloy, S. R. J. Brueck, N. C. Panoiu, and R. M. Osgood, "Near-infrared double negative metamaterials," *Opt. Express* **13**, 4922–4930 (2005).
19. V. M. Shalaev, W. Cai, U. K. Chettiar, H.-K. Yuan, A. K. Sarychev, V. P. Drachev, and A. V. Kildishev, "Negative index of refraction in optical metamaterials," *Opt. Lett.* **30**, 3356–3358 (2005).
20. M. Kafesaki, I. Tsiapa, N. Katsarakis, Th. Koschny, C. M. Soukoulis, and E. N. Economou, "Left-handed metamaterials: the fishnet structure and its variations," *Phys. Rev. B* **75**, 235114 (2007).
21. C. M. Soukoulis, S. Linden, and M. Wegener, "Negative

- refractive index at optical wavelengths,” *Science* **315**, 47–49 (2007).
22. J. Valentine, S. Zhang, T. Zentgraf, E. Ulin-Avila, D. A. Genov, G. Bartal, and X. Zhang, “Three-dimensional optical metamaterial with a negative refractive index,” *Nature* **455**, 376–380 (2008).
 23. A. Mary, S. G. Rodrigo, F. J. Garcia-Vidal, and L. Martin-Moreno, “Theory of negative-refractive-index response of double-fishnet structures,” *Phys. Rev. Lett.* **101**, 103902 (2008).
 24. R. Marques, L. Jelinek, F. Mesa, and F. Medina, “Analytical theory of wave propagation through stacked fishnet metamaterials,” *Opt. Express* **17**, 11582–11593 (2009).
 25. T. Koschny, M. Kafesaki, E. N. Economou, and C. M. Soukoulis, “Effective medium theory of left-handed materials,” *Phys. Rev. Lett.* **93**, 107402 (2004).
 26. J. Zhou, E. N. Economou, Th. Koschny, and C. M. Soukoulis, “Unifying approach to left-handed material design,” *Opt. Lett.* **31**, 3620–3622 (2006).
 27. D. R. Smith, S. Schultz, P. Markoš, and C. M. Soukoulis, “Determination of effective permittivity and permeability of metamaterials from reflection and transmission coefficients,” *Phys. Rev. B* **65**, 195104 (2002).
 28. K. B. Alici and Ekmel Ozbay, “A planar metamaterial: polarization independent fishnet structure,” *Photonics Nanostruct. Fundam. Appl.* **6**, 102–107 (2008).